

Progress in optical-field-ionization soft X-ray lasers at LOA*

T. MOCEK,¹ S. SEBBAN,¹ I. BETTAIBI,¹ Ph. ZEITOUN,¹ G. FAIVRE,¹ B. CROS,² G. MAYNARD,²
A. BUTLER,³ C.M. McKENNA,³ D.J. SPENCE,³ A.J. GONSAVLES,³ S.M. HOOKER,³
V. VORONTSOV,¹ S. HALLOU,¹ M. FAJARDO,⁴ S. KAZAMIAS,⁵ S. LE PAPE,⁶
P. MERCERE,¹ A.S. MORLENS,¹ C. VALENTIN,¹ AND Ph. BALCOU¹

¹Laboratoire d'Optique Appliquée (LOA), ENSTA-Ecole Polytechnique, Palaiseau, France

²Laboratoire de Physique des Gaz et des Plasmas, Université Paris-Sud, Orsay, France

³Department of Physics, University of Oxford, Oxford, United Kingdom

⁴Centro de Física dos Plasmas, Instituto Superior Técnico, Lisboa, Portugal

⁵Laboratoire d'Interaction du Rayonnement X avec la Matière, Université Paris-Sud, Orsay, France

⁶Laboratoire d'Utilisation des Lasers Intenses, Ecole Polytechnique, Palaiseau, France

(RECEIVED 30 September 2004; ACCEPTED 13 December 2004)

Abstract

We give an overview of recent advances in collisionally pumped optical field-ionization soft X-ray lasers developed at LOA. Saturated amplification has been achieved on the 5d-5p transition in Xe⁸⁺ at 41.8 nm, and on the 4d-4p transition in Kr⁸⁺ at 32.8 nm. We demonstrate a significant increase of the energy output from the Xe⁸⁺ laser driven within two types of wave-guide. Finally, we present results of a pioneering work aimed to set up and characterize the first true soft X-ray laser chain.

Keywords: Collisional excitation; Femtosecond; Guiding; High harmonic amplification; X-ray laser

1. INTRODUCTION

The advent of ultrashort laser technology has made it possible to employ relatively small-scale, femtosecond laser systems, working at high repetition rates as a pumping devices for bright X-ray sources (Mocek *et al.*, 2002; Faenov *et al.*, 2004; Fukuda *et al.*, 2004; Gavrilov *et al.*, 2004), and soft X-ray lasers (Ros *et al.*, 2002; Tallents *et al.*, 2002; Lan *et al.*, 2004). By focusing a femtosecond, terawatt laser beam into a gaseous medium, a multiply ionized, strongly non-equilibrium plasma can be produced by the optical-field-ionization (OFI) (Bauer, 2003), and population inversion between excited states of specific ionic species can be obtained. In the past few years, several inversion schemes for recombination and collisionally excited OFI soft X-ray lasers (SXRL) was proposed (Lemoff *et al.*, 1994), experimentally demonstrated (Nagata *et al.*, 1993; Chichkov *et al.*, 1995; Lemoff *et al.*, 1995; Sebban *et al.*, 2002), and characterized (Mocek *et al.*, 2004). For both classes of OFI SXRL,

the lifetime of the population inversion is very short, and so the pumping must be in the form of a traveling wave. This can be achieved most easily by longitudinal pumping. However, the most serious issue of the longitudinal pumping geometry is the formation of a sufficient length of plasma for amplification of the X-ray photons to occur, since the Rayleigh length naturally limits the length of the amplifying medium to at best a few millimeters. In order to extend the gain length that can be achieved by longitudinal pumping, it is necessary to guide the pump pulse over many Rayleigh lengths. Several techniques for guiding laser pulses with peak intensities relevant to OFI laser schemes, 10^{16} – 10^{18} W cm⁻², have been investigated. These include guiding in hollow capillaries, relativistic channeling, and various types of plasma wave-guide.

In this paper, we report on recent advances in collisional OFI SXRL using Pd-like and Ni-like ions. We present the experimental results to demonstrate driving a collisional OFI laser within the channels of two types of wave-guide: a capillary discharge plasma wave-guide, and a multi-mode, gas-filled capillary. We also will show results of a pioneering work toward the first true SXRL chain consisting of high harmonic seed and OFI plasma amplifier.

Address correspondence and reprint requests to: T. Mocek, Laboratoire d'Optique Appliquée (LOA), ENSTA-Ecole Polytechnique, Palaiseau, France.
E-mail: mocek@fzu.cz

*This paper was presented at the 28th ECLIM conference in Rome, Italy

2. LASING IN A GAS CELL

The experiments were performed at the Laboratoire d'Optique Appliquée (LOA) using a 10 Hz multi-terawatt Ti:Sapphire laser system (Pittman *et al.*, 2002), delivering 34 fs pulses (full width at half maximum), with an energy on target of up to 1 J. Figure 1 shows the typical experimental setup. The circularly polarized laser beam was focused onto the gas cell entrance, by a spherical mirror of focal length of 1 m or 2 m. The resulting maximum intensity on target was up to $(1 \pm 0.2) \times 10^{18} \text{ W cm}^{-2}$ in a vacuum. The polarization of the driving laser was adjustable by means of a 50-mm-diameter motorized quarter wave plate. The interaction medium was a static gas cell filled with Xe or Kr held at uniform pressure. At the beginning of each experimental session, two replaceable pinholes ($\sim 0.5 \text{ mm}$ in diameter) were drilled by the driving laser on both sides of the gas cell, to provide differential pumping and isolate the gas-filled and vacuum regions. The principal diagnostics was an on-axis soft X-ray transmission grating spectrometer, composed of a grazing incidence gold coated spherical mirror, transmission grating with 2000 lines/mm, and a back-illuminated X-ray charge-coupled device (CCD) camera. Stray light from the driving laser was blocked by two $0.3 \mu\text{m}$ -thick aluminum filters.

The easiest way to increase the length of SXRL amplifier and so to boost up the output signal is to employ a longer focal length optic (2 m instead of 1 m used in previous experiments), providing that the laser intensity is still above the threshold to generate Xe^{8+} or Kr^{8+} by OFI. Figure 2 shows calculated distribution of charge states following the passage of the pump laser pulse in a gas cell using focusing optics of 1 m and 2 m, respectively. As expected, the simulation predicts a significant elongation (up to 8 mm) of the amplifier length for the $f = 2 \text{ m}$ geometry. Figure 3 presents the measured SXRL signal at 41.8 nm as a function of the gas cell length using the 2 m focal length, focusing optics demonstrating a dramatic increase of the SXRL output for cell length of 8 mm. The lasing signal is about 13 times higher than that measured using $f = 1 \text{ m}$ focusing optics. While this geometry worked well for the Xe^{8+} laser, it was not appropriate for the Kr^{8+} laser at 32.8 nm as the

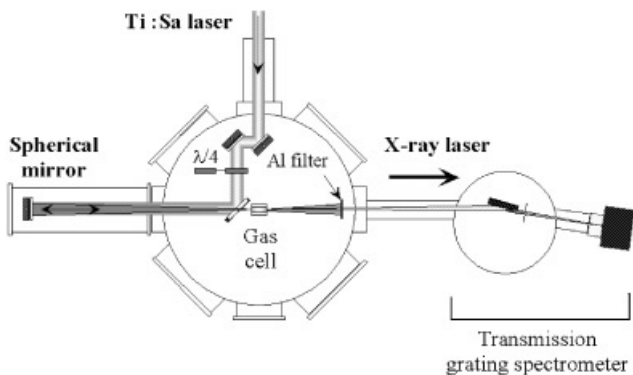


Fig. 1. Schematic of the experimental setup.

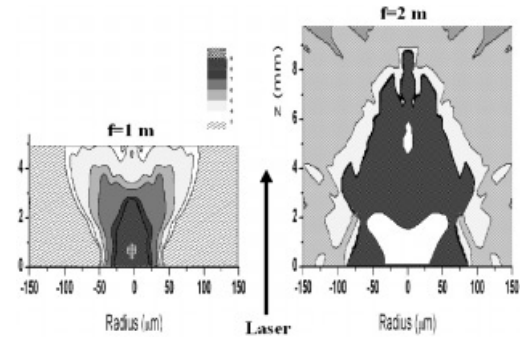


Fig. 2. Calculated distribution of Xe charge states following the passage of the pump laser pulse for the $f = 1 \text{ m}$ (left) focusing optics, and for the $f = 2 \text{ m}$ (right).

available driving laser intensity was insufficient to generate plasma column longer than 4 mm.

3. DRIVING THE Xe^{8+} LASER IN WAVE-GUIDES

3.1. Lasing in a plasma wave-guide

Figure 4 shows schematically the gas-filled capillary discharge wave-guide. When used purely as a wave-guide, a current pulse of several hundred Amperes, and duration of approximately $1 \mu\text{s}$, is discharged through a capillary filled with hydrogen gas (Butler *et al.*, 2002). The capillary discharge forms a plasma channel able to guide high intensity ($> 10^{17} \text{ W cm}^{-2}$) laser pulses over lengths of several centimeters. In order to drive a short-wavelength laser within the plasma channel, it is necessary to dope the hydrogen gas with the lasing gas. To enable comparison with earlier works, the wave-guide could be replaced with a 4 mm long gas cell, similar to that described by Sebban *et al.* (2003). The cell was positioned such that, in a vacuum, the pump beam was focused a few mm after the front pinhole.

Figure 5 compares the spectrum recorded with the gas cell containing pure Xe at the optimum pressure of 20 mbar

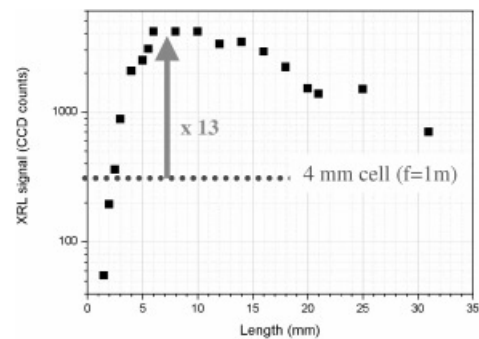


Fig. 3. Measured Xe^{8+} laser signal as a function of the gas cell length using $f = 2 \text{ m}$. The typical signal level obtained with $f = 1 \text{ m}$ is also shown.

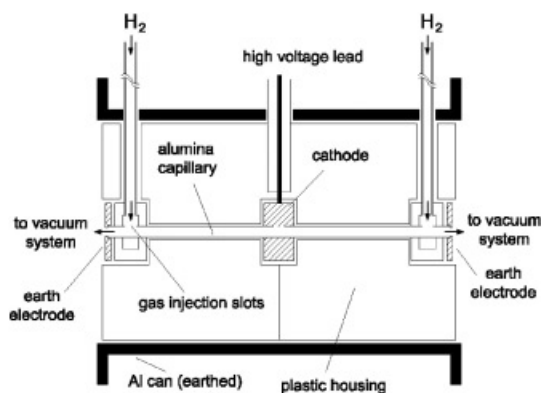


Fig. 4. Schematic diagram of a gas-filled capillary discharge wave-guide.

with the spectrum recorded using the wave-guide for the optimum conditions: 1:3 Xe:H atom gas mixture at an initial pressure of 120 mbar, and a delay $t = 1000$ ns. It is seen that for both the gas cell and wave-guide strong lasing occurred at 41.8 nm, the signal recorded with the wave-guide being approximately 4 times larger than achieved with the gas cell. The Xe^{8+} laser signal recorded with the capillary discharge wave-guide was found to depend critically on the delay at which the pump laser pulses were injected into the capillary, and to be closely correlated to the conditions required to achieve good guiding of the pump laser pulse (Butler *et al.*, 2003). As such, it was concluded that the Xe^{8+} lasing depended not only on the plasma conditions established by the discharge, but also on good guiding of the pump laser pulses over the 30 mm length of the wave-guide. The presence of hydrogen is expected to decrease the small-signal gain coefficient of the Xe^{8+} laser transition through partial pre-ionization of the Xe by the discharge, reduction of the gain cross-section resulting from the increased transition line width, and an increased rate of de-excitation of the laser levels. As a consequence, while the gain length of collisionally-excited OFI lasers can be greatly increased by

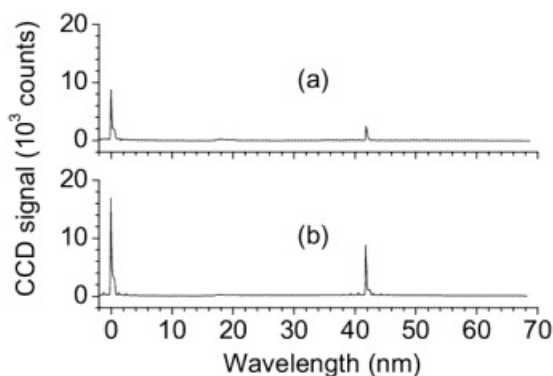


Fig. 5. The measured spectrum for (a) a gas cell (b) a Xe/H gas-filled capillary discharge wave-guide. The feature at “0 nm” is the zero-order.

driving them within a gas-filled capillary discharge plasma wave-guide, the single-pass gain may not be increased by the same factor.

3.2. Lasing in a multimode capillary tubes

We have also investigated an OFI SXRL driven on another type of wave-guide: a multi-mode, gas-filled capillary. In this case, the capillary is filled with pure lasing gas, and no discharge is employed. With this wave-guide, channeling of the laser pulse occurs as a result of reflection at the capillary wall. It is important to note that for these experiments, the spot radius of the pump pulse in the entrance plane of the capillary was approximately 10 times smaller than the capillary diameter, so the guiding is expected to be highly multi-mode. The capillaries used were 15 mm long, with an internal diameter of $300 \pm 10 \mu\text{m}$. Since the channels were laser machined, the walls of the capillaries were not optically smooth, but contained non-uniformities with typical dimensions of $5 \mu\text{m}$. Xe gas was flowed into the capillary through channels approximately $500 \mu\text{m}$ wide and $250 \mu\text{m}$ deep, located 1.5 mm from each end. By injecting the gas in this way, the pressure in the main body of the capillary between the gas slots was uniform.

Figure 6 compares optimized output signals from the cell at 17 Torr (squares) and the capillary at 17 Torr (solid triangles) as a function of target length. The position of the vacuum focus was 5 mm inside the cell (capillary). The solid curves represent the results of simplified modeling of the radiation transfer in the active medium, being in good agreement with the experimental results. The data clearly shows that the capillary greatly increases the lasing signal compared to that achieved with a gas cell. The strongest signal ever was observed with a 15 mm long capillary at 30 Torr, being nearly an order of magnitude higher than the largest signal achieved with the cell of the same length, and as much as 43 times higher than that with a 4 mm cell. In addition, the wave-guide allowed lasing to be achieved over a wider range of pressures, than in the gas cells.

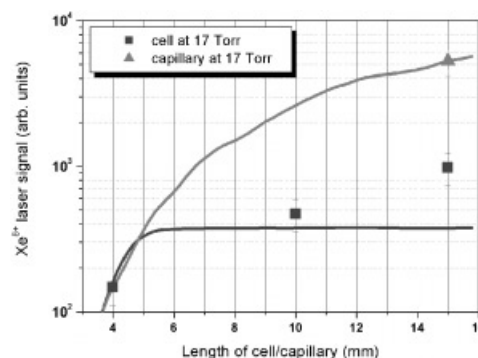


Fig. 6. Measured and simulated (solid lines) Xe^{8+} laser signal from the capillary (solid triangle) and the cell (squares) at 17 Torr as a function of the cell or capillary length.

Figure 7 shows the calculated distribution of Xe ion stages following the passage of the pump laser pulse through a 15 mm long cell (a) and capillary tube (b) under the conditions found experimentally to produce the largest Xe⁸⁺ laser signal, that is, a pressure of 17 Torr and a focusing position of 6 mm inside the cell. It is seen that Xe⁸⁺ is produced along the whole length of the capillary, in an annular region with higher ion stages, being generated in an approximately cylindrical region of radius $\sim 20 \mu\text{m}$ along most of the capillary axis. By comparing Figs. 7a and 7b, it appears that the region of Xe⁸⁺ is likely to be formed along the whole length of the capillary.

4. AMPLIFICATION OF HIGH ORDER HARMONICS IN OFI PLASMA

Although the optimized OFI SXRLs mentioned above provide up to 10^{11} photons per shot at 10 Hz, the optical quality of the generated beam is rather poor, with irregular wave front, weak coherence, and long pulse duration (~ 3 ps). The low quality of SXRL is caused by the fact that the self-emission is amplified (ASE) in a single pass along the laser medium without any filtering, thus generating an intense but noisy beam. The major improvement of the existing SXRL architecture thus consists in extrapolating the common architecture of visible lasers into soft X-ray region. In a classical laser chain, the oscillator delivers a pulse with perfect spectral, temporal, and spatial properties while the amplifier is used for increasing the beam energy. In X-ray region, high harmonic generation (HHG) can provide high quality pulses as required for the seed, while SXRL amplifying medium can be used as an amplifier stage.

Following this idea, we performed an experiment aimed at demonstration and characterization of the first true SXRL chain (Fig. 8). The X-ray amplifying laser chain was made of three parts: a HHG seed, a focusing system, and an OFI SXRL amplifier. Harmonics were produced by focusing a 20 mJ, 30 fs, infrared laser beam into a gas cell of variable pressure and length, filled with Ar or Xe. The major optimization was the fine adjustment of the wavelength of one

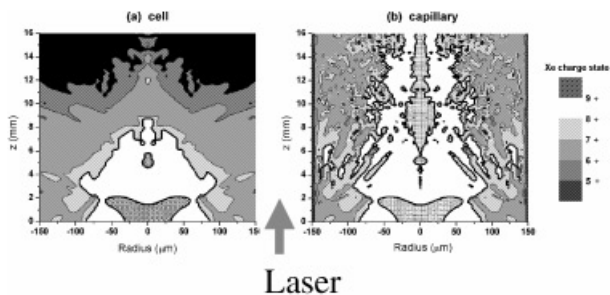


Fig. 7. Calculated distribution of Xe charge states following the passage of the pump laser pulse for a 15 mm long (a) cell, and (b) capillary. For both calculations the position of the vacuum focus was 6 mm inside the target, and the pressure was 17 Torr.

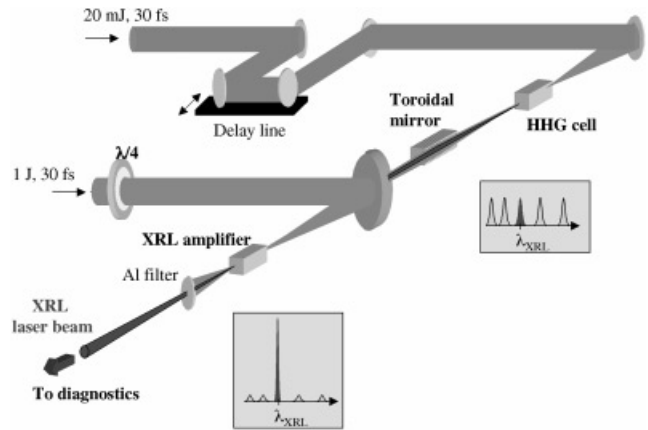


Fig. 8. Schematic description of the experimental setup for the first SXRL chain.

particular harmonic (25th or 19th), so as to coincide with the wavelength of the SXRL under investigation (32.8 nm or 41.8 nm), achieved by controlling the chirp of the infrared laser. The amplifying plasma was created by focusing a 1 J, 30 fs laser into another gas cell filled with lasant gas (Xe or Kr). The output of the harmonic source was re-imaged at the entrance of the amplifying plasma by means of grazing incidence toroidal mirror. The output X-ray beam was analyzed by an on-axis soft X-ray spectrometer or by a monochromatic foot-print monitor consisting of a removable 45°, soft X-ray interferential multilayer mirror (Mo/B₄C/Si) which sent the beam onto a cooled, thin, back-illuminated CCD.

When the HHG seed was synchronized with the maximum gain of the SXRL amplifier, a strong amplification has been observed. Figure 9 displays experimental spectra corresponding to (a) HHG alone, (b) Kr⁸⁺ SXRL alone, (c) SXRL with HHG seeding long after gain extinction, and (d) HHG synchronized with maximum SXRL gain. The ampli-

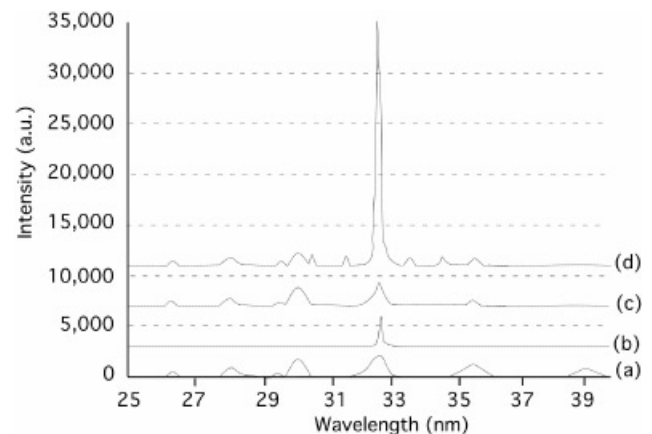


Fig. 9. Experimental spectra under conditions: (a) HHG only, (b) SXRL only, (c) both HHG and SXRL non-synchronized, and (d) the amplified seeded SXRL.

fication period starts typically 2–5 ps after the interaction of the IR laser with the gas and lasts for several ps depending on gas density. Figure 9d clearly shows that strong amplification of the HHG seed has been achieved. In this case, HHG were seeded at about twice the intensity of the ASE of the SXRL, leading to an enhancement of the output signal by a factor of 13. It was found that seeding a SXRL with a HHG source with a much wider bandwidth is extremely beneficial for energy extraction, because ions with stimulated transitions that are normally spectrally shifted too far to amplify incident radiation, may now participate in the amplification. The seeded SXRL provides currently $\sim 1.5 \times 10^{11}$ (0.8 μJ) photons per pulse in a narrowly collimated beam with divergence of as little as 1 mrad. The generated beam is linearly polarized and possesses high degree of spatial coherence. Due to the strong saturation, the estimated Fourier-limited pulse duration of the amplified seed amounts to approximately 500 fs. Assuming a focal spot close to the diffraction-limit (0.1 μm), such a seeded SXRL has a potential to achieve intensities as high as $10^{16} \text{ W cm}^{-2}$, and to become a key tool in the emerging applications such as structural biology and warm dense matter.

5. CONCLUSIONS

In conclusion, we have demonstrated that wave-guides may be employed to increase significantly the output energy of collisionally excited OFI SXRLs. The Xe^{8+} laser at 41.8 nm driven in a multi-mode, gas-filled capillary provides up to 1.5×10^{11} photons/pulse (0.8 μJ) at 10 Hz, in 4 mrad of divergence. In an alternative approach, by combining the high optical quality available from HHG with an energetic OFI SXRL amplifier, we produced the first high-intensity, femtosecond, fully polarized and highly coherent SXRL at 41.8 nm and 32.8 nm operating at 10 Hz.

ACKNOWLEDGMENTS

The authors acknowledge invaluable technical support from the laser staff at the Laboratoire d'Optique Appliquée. T. Mocek was supported by a Marie Curie Individual Fellowship of the European Commission and S.M. Hooker by a Royal Society University Research Fellowship. This work was partly supported by the European Community—Access to Research Infrastructure action of the Improving Human Potential Program.

REFERENCES

- BAUER, D. (2003). Plasma formation through field ionization in intense laser–matter interaction. *Laser Part. Beams* **21**, 489–495.
- BUTLER, A., GONSALVES, A.J., MCKENNA, C.M., SPENCE, D.J., HOOKER, S.M., SEBBAN, S., MOCEK, T., BETTAIBI, I. & CROS, B. (2003). Demonstration of a collisionally excited optical-field-ionization XUV laser driven in a plasma wave-guide. *Phys. Rev. Lett.* **91**, 205001.
- BUTLER, A., SPENCE, D.J. & HOOKER, S.M. (2002). Guiding of high-intensity laser pulses with a hydrogen-filled capillary discharge wave-guide. *Phys. Rev. Lett.* **89**, 185003.
- CHICKOV, B.N., EGBERT, A., EICHMANN, H., MOMMA, C., NOLTE, S. & WELLEGEHAUSEN, B. (1995). Soft-X-ray lasing to the ground states in low-charged oxygen ions. *Phys. Rev. A* **52**, 1629–1639.
- FAENOV, A., PIKUZ, T., MAGUNOV, A., BATANI, D., LUCCHINI, G., CANOVA, F. & PISELLI, M. (2004). Bright, point X-ray source based on commercial portable 40 ps Nd:YAG laser system. *Laser Part. Beams* **22**, 373–379.
- FUKUDA, Y., AKAHANE, Y., AOYAMA, M., INOUE, N., UEDA, H., KISHIMOTO, Y., YAMAKAWA, K., FAENOV, YA., MAGUNOV, A.I., PIKUZ, T.A., SKOBELEV, I.YU., ABDALLAH, J., CSANAK, G., BOLDAREV, A.S. & GASILOV, V.A. (2004). Generation of X-rays and energetic ions from superintense laser irradiation of micron sized Ar clusters. *Laser Part. Beams* **22**, 215–220.
- GAVRILOV, S.A., GOLISHNIKOV, D.M., GORDIENKO, V.M., SAVEL'EV, A.B. & VOLKOV, R.V. (2004). Efficient hard X-ray source using femtosecond plasma at solid targets with a modified surface. *Laser Part. Beams* **22**, 301–306.
- LAN, K., FILL, E. & MEYER-TER-VEHN, J. (2004). Photo pumping of XUV lasers by XFEL radiation. *Laser Part. Beams* **22**, 261–266.
- LEMOFF, B.E., BARTY, C.P.J. & HARRIS, S.E. (1994). Femtosecond-pulse-driven, electron-excited XUV lasers in 8-times-ionized noble gases. *Opt. Lett.* **19**, 569–571.
- LEMOFF, B.E., YIN, G.Y., GORDON III, C.L., BARTY, C.P.J. & HARRIS, S.E. (1995). Demonstration of a 10-Hz femtosecond pulse-driven XUV laser at 41.8 nm in Xe IX. *Phys. Rev. Lett.* **74**, 1574–1577.
- MOCEK, T., KIM, C.M., SHIN, H.J., LEE, D.G., CHA, Y.H., HONG, K.H. & NAM, C.H. (2002). Investigation of soft X-ray emission from Ar clusters heated by ultrashort laser pulses. *Laser Part. Beams* **20**, 51–57.
- MOCEK, T., SEBBAN, S., BETTAIBI, I., UPCRAFT, L.M., BALCOU, P., BREGER, P., ZEITOUN, P., LE PAPE, S., ROS, D., KLISNICK, A., CARILLON, A., JAMELOT, G., RUS, B. & WYART, J.F. (2004). Characterization of collisionally pumped optical-field-ionization soft X-ray lasers. *Appl. Phys. B* **78**, 939–944.
- NAGATA, Y., MIDORIKAWA, K., KUBODERA, S., OBARA, M., TASHIRO, H. & TOYODA, K. (1993). Soft-X-ray amplification of the Lyman-alpha transition by optical-field-induced ionization. *Phys. Rev. Lett.* **71**, 3774–3777.
- PITTMAN, M., FERRÉ, S., ROUSSEAU, J.P., NOTEBAERT, L., CHAMBARET, J.P. & CHÉRIAUX G. (2002). Design and characterization of a near-diffraction-limited femtosecond 100-TW 10-Hz high-intensity laser system. *Appl. Phys. B* **74**, 529–535.
- ROS, D., JAMELOT, G., CARILLON, A., JAEGLE, P., KLISNICK, A., ZEITOUN, P., RUS, B., JOYEUX, D., PHALIPPOU, D., BOUS-SOUKAYA, M., ZEITOUN-FAKIRIS, A., ALBERT, F., FOURCADE, P., HUBERT, S., SEBBAN, S., LAGRON, J.C. & VANBOSTAL, L. (2002). State of the development of X-ray lasers and applications at LSAI. *Laser Part. Beams* **20**, 23–30.
- SEBBAN, S., MOCEK, T., ROS, D., UPCRAFT, L.M., BALCOU, P., HAROUTUNIAN, R., GRILLON, G., RUS, B., KLISNICK, A., CARILLON, A., JAMELOT, G., VALENTIN, C., ROUSSE, A., ROUSSEAU, J.P., NOTEBAERT, L., PITTMAN, M. & HULIN, D. (2002). Demonstration of a Ni-like Kr optical-field-ionization collisional soft X-ray laser at 32.8 nm. *Phys. Rev. Lett.* **89**, 253901.

- SEBBAN, S., UPCRAFT, L.M., BALCOU, P., PITTMAN, M., HAROUTUNIAN, R., GRILLON, G., VALENTIN, C., ROUSSE, A., ROUSSEAU, J.P., NOTEBAERT, L., HULIN, D., MOCEK, T., RUS, B., ROS, D., KLISNICK, A., CARILLON, A. & JAMELOT, G. (2003). Investigations of collisionally pumped optical field ionization soft-X-ray lasers. *J. Opt. Soc. Am. B* **20**, 195–202.
- TALLENTS, G.J., ABOU-ALI, Y., EDWARDS, M., KING, R., PERT, G.J., PESTEHE, S.J., STRATI, F., LEWIS, C.L.S., KEENAN, R., TOPPING, S., KLISNICK, A., GUILBAUD, O., ROS, D., CLARKE, R., NOTLEY, M. & NEELY, D. (2002). A review of X-ray laser development at Rutherford Appleton Laboratory. *Laser Part. Beams* **20**, 201–209.